Organization of polyene antibiotic amphotericin B at the argon-water interface

Mariusz Gagoś, Wieslaw I. Gruszecki

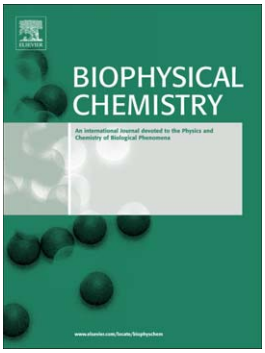

Organization of polyene antibiotic amphotericin B at the argon-water interface

Mariusz Gagoś, Wiesław I. Gruszecki

PII: S0301-4622(08)00161-0
DOI: doi: 10.1016/j.bpc.2008.08.001
Reference: BIOCHE 5141

To appear in: *Biophysical Chemistry*

Received date: 30 May 2008
Revised date: 1 August 2008
Accepted date: 2 August 2008

Please cite this article as: Mariusz Gagoś, Wiesław I. Gruszecki, Organization of polyene antibiotic amphotericin B at the argon-water interface, *Biophysical Chemistry* (2008), doi: 10.1016/j.bpc.2008.08.001

Organization of polyene antibiotic amphotericin B at the argon-water interface

Mariusz Gagoś[1,2] and Wiesław I. Gruszecki[1*]

1. Department of Biophysics, Institute of Physics, Maria Curie-Skłodowska University, 20-031 Lublin, Poland
2. Department of Physics, University of Life Science, 20-033 Lublin, Poland

Key words: polyene antibiotics; amphotericin B; membrane channels; molecular aggregates, excitonic interactions; monomolecular films; linear dichroism

Corresponding author:
Wiesław I. Gruszecki
Department of Biophysics
Institute of Physics
Maria Curie-Skłodowska University
20-031 Lublin, Poland
Fax: +(48 81) 537 61 91, Phone: +(48 81) 537 62 52
E-mail:wieslaw.gruszecki@umcs.pl

Abstract

Amphotericin B (AmB) is a life-saving antibiotic, used to treat deep-seated mycotic infections. Both the therapeutic and toxic side effects of AmB are directly dependent on its molecular organization. Organization of AmB was studied in monocomponent monomolecular layers formed at the argon-water interface, by means of polarized and non-polarized electronic absorption spectroscopy and analyzed in terms of the exciton splitting theory. The results provide direct indication that AmB forms spontaneously dimers that can be assembled into molecular structures characterized by homogeneous orientational distribution in the monolayer, interpreted as cylindrical pores. The structures are not stable at surface pressures higher than 20 mN/m and therefore dimers are concluded as abundant molecular organization forms of AmB in biomembranes. Possibility of stabilization of the cylindrical structures, at higher surface pressures, by other molecules, eg. sterols, is also discussed.

Introduction

Amphotericin B (AmB) is a macrolide poliene antibiotic (Fig. 1) popular in treatment of deep-seated mycotic infections [1-3]. AmB has been in use for almost fifty years and despite its strong side effects is still popular as a life saving antibiotic. It is generally accepted that the biological effect of AmB is based upon interaction to cellular membranes but detailed molecular mechanisms responsible for both pharmacological as well as toxic side effects are still not fully understood. The most popular concept regarding the effect of AmB on biomembranes is directly associated with formation of transmembrane pores that are able to affect severely the physiological ion transport [4]. The ability of AmB molecules to form cylindrical structures that can play possibly the role of membrane pores, gained support from the theoretical studies carried out with application of the electrostatic interaction analysis [5], molecular dynamics approach [6-8] and from the experimental studies on ion permeability [9]. The ability of AmB to form ring-shaped molecular aggregates has been demonstrated by the scanning force microscopic analysis of monomolecular layers of the drug [10]. On the other hand, the results of recent experiments carried out with application of the ^{1}H-NMR [11] and FTIR [12] techniques demonstrated that the principal site of localization of AmB with respect to the lipid membrane is the polar headgroup region. The results of the linear dichroism analysis of orientation of AmB molecules in the lipid membranes were interpreted in terms of existence of two pools of AmB, one parallel and one perpendicular with respect to the plane of the lipid bilayer [13, 14]. Interestingly, it was documented that low molar fractions of AmB (below 1 mol% with respect to lipid) increased the barrier for the transmembrane proton transport and the transport was facilitated only at higher concentrations of the drug, that promote formation of aggregated structures [15]. Such a finding correlates with the results reported recently, according to which AmB present in the lipid membrane system, at the concentrations higher than 1 mol%, aggregates and is able to penetrate the

hydrophobic membrane core [16]. Despite those recent reports the question still remains open whether AmB molecules which penetrate the hydrophobic core of the lipid membrane, form cylindrical aggregates (pores) or remain in the form of small molecular aggregates e.g. dimers. Very efficient formation of dimeric structures by AmB has been predicted on the basis of the theoretical analysis of molecular interactions [17] and has been demonstrated with application of electronic absorption and fluorescence spectroscopic analyses [13, 18-20]. The formation of AmB dimers has been also concluded on the basis of monomolecular layer studies [21]. In the present work we address the problem of molecular organization of AmB using electronic absorption spectroscopy with non-polarized and polarized light and monomolecular layer technique. Our results show efficient formation of dimers of AmB which, under certain conditions, may be assembled into the symmetrical molecular forms interpreted as cylindrical pores. Such structures of AmB, formed in the environment of biomembranes are able to disturb severely physiological ion transport and are believed to be responsible for pharmaceutical activity of the drug. The analysis of the spectral shifts have been very frequently applied to study molecular organization of AmB [22-36]. The approach applied in the present work enables to link the spectral changes in the electronic absorption spectra with defined molecular organization patterns.

Materials and methods

Amphotericin B (AmB) in a crystalline form was purchased from Sigma Chem. Co. AmB was dissolved in 40% 2-propanol and then centrifuged for 15 min at 15 000 x g in order to remove micro crystals of the drug still remaining in the sample. AmB was further purified by means of HPLC on YMC C-30 coated phase reversed column (length 250 mm, internal diameter 4.6 mm) with 40% 2-propanol in H_2O as a mobile phase. The final concentration of AmB was

calculated from the absorption spectra on the basis of the molar extinction coefficient 1.3 x 10^5 $M^{-1}cm^{-1}$ in the 0-0 absorption maximum at 408 nm. Monomolecular layers of the AmB were formed at the argon-water interface. As a first step, AmB solution was deposited at many places of the interface. Monolayers were formed on mQ water. Monomolecular layers were formed in a Teflon trough 40 cm x 4 cm and were compressed along the long side with the speed of 4.8 cm^2/min. Surface pressure was monitored by NIMA Technology tensiometer, model PS3 (Coventry, England). Monolayer compression, surface pressure measurements and data acquisition were controlled by our own software. Monolayers compression was carried out at 25 ± 1 ^oC. Detailed analysis of formation of monomolecular layers of AmB was presented by us previously [10, 12, 37]. Light absorption measurements and linear dichroism measurements were carried out with a Diode array UV–Vis spectrophotometer HP 8453. Glan-Taylor polarizer was used in the polarization experiments (Fig. 2). Spectral analysis was performed with Grams/AI software from ThermoGalactic (USA). During compression of AmB monolayers, desorption of molecules from the interface into the subphase was not observed before the monolayer collapse, as concluded on the basis of absorbance measurements of the subphase medium. To assure that AmB desorbed into the aqueous phase do not interfere with the spectroscopic measurements of monomolecular layers each experiment was performed with the freshly prepared subphase.

Results and discussion

Fig. 3 presents the isotherm of compression of the monomolecular film formed with AmB at the argon-water interface. The shape of the isotherm represents a two phase process, as can be deduced from two distinct linear portions of the isotherm of compression, corresponding to the specific molecular areas of 148 $Å^2$/molecule and 36 $Å^2$/molecule [38]. These values of the specific area correspond to different orientation of AmB at the argon-water interface, most

probably the horizontal at low surface pressure values and vertical with AmB anchored in the subphase with mycosamine polar head [12, 14, 37, 39] (see inset to Fig. 3). The specific molecular area of 36 $Å^2$/molecule is close to the theoretical cross-section of AmB (approximately 6 Å x 7 Å) [5] and therefore indicates tight molecular packing of the monolayer at high surface pressures, despite the amphiphilic character of the AmB molecule. The relatively high pressure of collapse, close to 45 mNm^{-1}, is an indication that such structures are relatively stable and can be also stable in lipid biomembranes (30-35 mN/m [39-41]). Characteristic plateau phase in the molecular area range 100 $Å^2$ to 40 $Å^2$ corresponds to the reorientation of AmB molecules at the interface [10, 12, 37]. Fig. 4 presents the electronic absorption spectra of the AmB monolayer recorded during compression, at different surface pressures: 0, 25 and 32 mN/m. AmB molecules deposited at the argon-water interface display typical light absorption spectrum, characteristic of the antibiotic in monomeric form [13], with characteristic vibrational bands peaking at 409, 385 and 364 nm (see Tab. I). Gaussian analysis of the absorption spectrum shows that even in the beginning of compression, the molecules of AmB deposited at the argon-water interface, interact one to each other, as can be deduced from the spectral broadening represented by the minor Gaussian components visible in the red edge of the spectrum as well as in the short wavelength spectral region. This effect can be particularly observed at higher surface pressure values. The absorption spectrum of the AmB monolayer compressed to the surface pressure 32 mN/m demonstrates pronounced hypsochromic shift, typical of the card-pack aggregates of AmB [13, 24, 34], formed also in the lipid phase [11, 13, 14]. Both the short- as well as the long-wavelength spectral shifts of the absorption spectrum of AmB can be observed in the absorption spectrum recorded at the surface pressure 25 mN/m. Such a spectral feature, along with a distinct vibrational substructure of the spectrum, suggests that excitonic interactions which give rise to the spectral shifts observed, are associated with formation of small

molecular aggregates, most probably dimers, with oblique orientation of the dipole moments of the neighboring molecules. The excitonic interactions accompanying formation of molecular aggregates [42] are manifested by spectral shifts that can be described, within the framework of the exciton splitting theory, by the following dependency [43]:

$$\nu_m = \nu_{mon} + 2\beta\cos\left(\frac{m\pi}{N+1}\right) \quad (1)$$

where ν_m is the position of the m-th excitation state in the spectrum of the aggregated form, ν_{mon} is the position of the electronic transition in the spectrum of monomeric chromophores, N is a number of all exciton states and m is the number of the exciton state considered. In the case of a maximum hypsochromic shift m=1. β is a dipole-dipole coupling matrix element [43] and is expressed as:

$$\beta = \frac{|\mu_{mon}|^2}{4\pi\varepsilon_o n^2 R^3}\left(\cos\theta - 3\cos^2\nu\right) \quad (2)$$

In the formula μ_{mon} is a dipole transition moment of a monomer, ε_o is the dielectric permittivity of vacuum, n is the refractive index of the medium and R is the distance between the centers of the transition dipoles of the nearest neighbors in the aggregate. The angle between monomeric transition moment vectors, θ, and the angle between the transition moment vector and the axis connecting the centers of the transition moment vectors of neighboring molecules, ν, were assumed to be 0^o and 90^o, respectively, in the case of H-aggregates of AmB (neighboring molecules are parallel one to each other and perpendicular to the plane of aggregation). A value of 11.3 Debye for the transition dipole of monomeric AmB

was calculated based on the integration of the absorption spectra. Analysis of the spectral components of AmB monolayer compressed to 25 mN/m (see Tab. I) indicates that the principal absorption bands are symmetrically shifted both towards the lower and the higher energies by two different values of β termed β_1 (890 cm^{-1}) and β_2 (3741 cm^{-1}). Despite very low level of absorbance of a single monomolecular layer of AmB and some differences in proportions of intensity of the spectral bands recorded, both the bathochromic and hypsochromic spectral shifts observed in course of film compression were highly reproducible in all repetition of the experiment. The analysis of possible molecular arrangements based on Eq. 2 let us to conclude that in the case of β_1 the chromophores (dipole transitions) of neighboring molecules are separated by less than 7.4 Å and in the case of β_2 by less than 4.4 Å. It is therefore possible that both interaction energy values correspond to one molecular organization pattern in which the hydrophobic portions of neighboring AmB molecules interact one to each other by van der Waals forces (a short distance between the chromophores, R_2) and polar sides of the neighboring AmB molecules are linked by the hydrogen bonding (a long distance between the chromophores, R_1). The energy level diagram corresponding to the spectral shifts observed and possible molecular organization of AmB leading to the observed excitonic interaction is presented in Fig. 5. The analysis of the absorption spectrum of AmB in the monomolecular layer compressed to 25 mN/m fits exceptionally well to the dimeric organization of the molecules. Comparison of the intensity of the absorption bands corresponding to the monomeric form of AmB (409 nm) and to the dimeric spectral form (353 nm [13, 20]) enables an analysis of formation of molecular dimers in course of the monolayer compression (Fig. 6). The surface pressure dependency of the absorbance ratio $A_{409/353}$ is presented in Fig. 6C, as superimposed on the isotherm of compression. Interestingly, the comparison shows that dimerization of AmB, represented as the dimer to monomer ratio, does not follow exactly the compression of the layer, represented

by the mean area per molecule. In particular, the compression-induced reorientation of molecules, from the horizontal to the vertical position, observed at the surface pressures between 5 and 15 mN/m, is not associated with pronounced change in the monomer to dimer ratio. This means that molecular dimers of AmB are formed spontaneously at 0 and very low surface pressure values and that dimers, like monomers, are reoriented in the course of compression and take part in formation of higher molecular aggregates. A pronounced, surface pressure-induced dimerization of AmB, begins in the monomolecular layer when practically all molecules are oriented vertically and are located relatively close one to each other (mean molecular area below 90 $Å^2$).

The absorption spectra of AmB in the monomolecular layers subjected to the compression were also recorded with polarized light. Fig. 7 presents the surface pressure dependency of the absorbance level at 409 nm (where all the spectral forms absorb, including monomers, dimers and large aggregates) recorded with polarized light, with the electric vector of radiation polarized parallel ($A_{\parallel}$) and perpendicular ($A_{\perp}$) with respect to the direction of the compression (see Fig. 2B for the geometry of the measurements). The dichroic ratio R can be represented by the average orientation angle (Φ) of the projection of the transition dipole μ on the plane of the surface of the monolayer and the compression direction:

$$R = \frac{A_{II}}{A_{\perp}} = \frac{\langle \sin^2 \phi \rangle}{\langle \cos^2 \phi \rangle} = \frac{1}{\langle \cos^2 \phi \rangle} - 1 \qquad (3)$$

Fig. 7B presents the surface pressure dependency of the average $\cos^2\Phi$. A change of this value reflects compression-induced reorganization of AmB molecules in the monolayer. Interestingly, the first pronounced phase of molecular reorganization of AmB begins directly after the beginning of the monolayer compression, at relatively low surface pressures.

Essentially, no average horizontal orientation changes during molecules reorientation at the interface were observed (surface pressures 5-15 mN/m). As can be seen from Fig. 7B, very pronounced phase of ordering of AmB molecules in the monolayer (between 16-19 mN/m) corresponds to the massive dimerization of the molecules, as deduced from the analysis of Fig. 6. Very interestingly, such an organization phase leads to the $<\cos^2\Phi>$ value of 0.5, which is diagnostic of totally homogenous horizontal distribution of the AmB transition dipoles and may represent formation of symmetrical cylindrical structures interpreted as molecular pores (Fig. 7B, inset a). The formation of such structures in the monomolecular layers has been observed in the monomolecular layers, by means of scanning force microscopic analysis [10].

The structures formed during compression become decomposed ("broken", Fig. 7B, inset b) upon further compression of the monolayer (value of $<\cos^2\Phi>$ drops down). The fact that symmetrically-ordered structures of AmB are not stable at the surface pressures above 20 mN/m implies that dimer is the most abundant form of organization of the drug in natural biomembranes and suggests possible role of sterols in stabilization of molecular porous aggregated structures at higher surface pressures [33, 44].

The approach applied in the present work to record absorption spectra of AmB in the monomolecular layers in situ, under the conditions of controlled molecular distance (compression to selected surface pressure values) enabled, for the first time, to analyze the effect of the molecular organization of the drug on shape of the spectrum. The analyses of the spectral shifts have been very frequently applied to study molecular organization of AmB [22-36] but the present work links directly numerous spectral bands observed with the organization patterns of chromophores (dimers, large aggregates). Such elaboration will be helpful to carry future spectroscopic analyses of molecular organization of antibiotic amphotericin B in model lipid membranes and natural biomembranes and also to reanalyze

the spectroscopic data already published. The results of the experiments presented show directly ability of AmB to form two type of dimers characterized by different distance between chromophores, as concluded on the basis of the analysis of bathochromic and hypsochromic spectral shifts. Moreover, the data analysis suggests that the large molecular aggregates of the antibiotic are formed out of dimers as intermediate constituents. This particular finding can serve as a indication and suggestion to focus on molecular mechanisms responsible for AmB dimerization, in future studies on biological action of this antibiotic.

Acknowledgements

This research was financed by the Ministry of Education and Science of Poland from the budget founds for science in the years 2004-2007 within the research project 2P05F04327.

References

[1] M. Baginski, B. Cybulska, W.I. Gruszecki, Interaction of Macrolide Antibiotics with Lipid Membranes, in: A. Ottova-Liu (Ed.), Advances in Planar Lipid Bilayers and Liposomes, vol. 3, Elsevier Science Publ., Amsterdam, 2006, pp. 269-329.

[2] S. Hartsel, J. Bolard, Amphotericin B: new life for an old drug, Trends Pharmacol. Sci. 17 (1996) 445-449.

[3] R. Martinez, An update on the use of antifungal agents, J Bras Pneumol 32 (2006) 449-460.

[4] B. De Kruijff, R.A. Demel, Polyene antibiotic-sterol interaction in membranes of Acholeplasma Laidlawii cells and lecithin liposomes; III Molecular structure of the polyene antibiotic-cholesterol complex, Biochim. Biophys. Acta 339 (1974) 57-70.

[5] M. Bonilla-Marin, M. Moreno-Bello, I. Ortega-Blake, A microscopic electrostatic model for the amphotericin B channel, Biochim. Biophys. Acta 1061 (1991) 65-77.

[6] M. Baginski, J. Czub, K. Sternal, Interaction of amphotericin B and its selected derivatives with membranes: molecular modeling studies, Chem Rec 6 (2006) 320-332.

[7] M. Baginski, H. Resat, E. Borowski, Comparative molecular dynamics simulations of amphotericin B-cholesterol/ergosterol membrane channels, Biochim. Biophys. Acta 1567 (2002) 63-78.

[8] M. Baginski, H. Resat, J.A. McCammon, Molecular properties of amphotericin B membrane channel: a molecular dynamics simulation, Mol. Pharmacol. 52 (1997) 560-570.

[9] B.V. Cotero, S. Rebolledo-Antunez, I. Ortega-Blake, On the role of sterol in the formation of the amphotericin B channel, Biochim. Biophys. Acta 1375 (1998) 43-51.

[10] W.I. Gruszecki, M. Gagos, P. Kernen, Polyene antibiotic amphotericin B in monomolecular layers: spectrophotometric and scanning force microscopic analysis, FEBS Lett 524 (2002) 92-96.

[11] J. Gabrielska, M. Gagos, J. Gubernator, W.I. Gruszecki, Binding of antibiotic amphotericin B to lipid membranes: a 1H NMR study, FEBS Lett 580 (2006) 2677-2685.

[12] M. Gagos, J. Gabrielska, M. Dalla Serra, W.I. Gruszecki, Binding of antibiotic amphotericin B to lipid membranes: Monomolecular layer technique and linear dichroism-FTIR studies, Molec. Memb. Biol. 22 (2005) 433-442.

[13] W.I. Gruszecki, M. Gagos, M. Herec, Dimers of polyene antibiotic amphotericin B detected by means of fluorescence spectroscopy: molecular organization in solution and in lipid membranes, J. Photochem. Photobiol. B: Biol. 69 (2003) 49-57.

[14] W.I. Gruszecki, M. Gagos, M. Herec, P. Kernen, Organization of antibiotic amphotericin B in model lipid membranes. A mini review, Cell. Mol. Biol. Lett. 8 (2003) 161-170.

[15] M. Herec, H. Dziubinska, K. Trebacz, J.W. Morzycki, W.I. Gruszecki, An effect of antibiotic amphotericin B on ion transport across model lipid membranes and tonoplast membranes, Biochem. Pharmacol. 70 (2005) 668-675.

[16] M. Herec, A. Islamov, A. Kuklin, M. Gagos, W.I. Gruszecki, Effect of antibiotic amphotericin B on structural and dynamic properties of lipid membranes formed with egg yolk phosphatidylcholine, Chem Phys Lipids 147 (2007) 78-86.

[17] J. Caillet, J. Berges, J. Langlet, Theoretical study of the self-association of amphotericin B, Biochim. Biophys. Acta 1240 (1995) 179-195.

[18] W.I. Gruszecki, M. Herec, Dimers of polyene antibiotic amphotericin B, J. Photochem. Photobiol. B: Biol. 72 (2003) 103-105.
[19] R. Stoodley, K.M. Wasan, D. Bizzotto, Fluorescence of amphotericin B-deoxycholate (fungizone) monomers and aggregates and the effect of heat-treatment, Langmuir 23 (2007) 8718-8725.
[20] M. Gagos, M. Herec, M. Arczewska, G. Czernel, M. Dalla Serra, W.I. Gruszecki, Anomalously high aggregation level of the polyene antibiotic amphotericin B in acidic medium: Implications for the biological action, Biophys. Chem. (2008).
[21] M. Saint-Pierre-Chazalet, C. Thomas, M. Dupeyarat, C.M. Gary-Bobo, Amphotericin B-Sterol Complex formation and competition with egg phosphatidylcholine: A Monolayer Study, Biochim. Biophys. Acta 944 (1988) 477-486.
[22] J. Milhaud, V. Ponsinet, M. Takashi, B. Michels, Interactions of the drug amphotericin B with phospholipid membranes containing or not ergosterol: new insight into the role of ergosterol, Biochim Biophys Acta 1558 (2002) 95-108.
[23] H. Rinnert, C. Thirion, G. Dupont, J. Lematre, Structural studies on aqueous and hydroalcoholic solutions of a polyene antibiotic: Amphotericin B, Biopolymers 16 (1977) 2419-2427.
[24] J. Barwicz, W.I. Gruszecki, I. Gruda, Spontaneous organization of amphotericin B in aqueous medium, J. Colloid Interf. Sci. 158 (1993) 71-76.
[25] M. Gagos, R. Koper, W.I. Gruszecki, Spectrophotometric analysis of organisation of dipalmitoylphosphatylcholine bilayers containing the polyene antibiotic amphotericin B, Biochim. Biophys. Acta 1511 (2001) 90-98.
[26] F. Gaboriau, M. Cheron, L. Leroy, J. Bolard, Physico-chemical properties of the heat-induced 'superaggregates' of amphotericin B, Biophys. Chem. 66 (1997) 1-12.
[27] P.L. Hargreaves, T.S. Nguyen, R.O. Ryan, Spectroscopic studies of amphotericin B solubilized in nanoscale bilayer membranes, Biochim Biophys Acta 1758 (2006) 38-44.
[28] R.P. Hemenger, T. Kaplan, L.J. Gray, Structure of Amphotericin B Aggregates Based on Calculations of Optical Spectra, Biopolymers 22 (1983) 911-918.
[29] J. Mazerski, J. Bolard, E. Borowski, Effect of the modifications of ionizable groups of amphotericin B on its ability to form complexes with sterols in hydroalcoholic media, Biochim Biophys Acta 1236 (1995) 170-176.
[30] J. Mazerski, J. Grzybowska, E. Borowski, Influence of net charge on the aggregation and solubility behaviour of amphotericin B and its derivatives in aqueous media, Eur Biophys J 18 (1990) 159-164.
[31] J. Barwicz, I. Gruda, P. Tancrede, A kinetic study of the oxidation effects of amphotericin B on human low-density lipoproteins, FEBS Lett. 465 (2000) 83-86.
[32] J. Bolard, P. Legrand, F. Heitz, B. Cybulska, One-sided action of amphotericin B on cholesterol-containing membranes is determined by its self-association in the medium, Biochemistry 30 (1991) 5707-5715.
[33] C. Charbonneau, I. Fournier, S. Dufresne, J. Barwicz, P. Tancrede, The interactions of amphotericin B with various sterols in relation to its possible use in anticancer therapy, Biophys Chem 91 (2001) 125-133.
[34] P. Tancrede, J. Barwicz, S. Jutras, I. Gruda, The effect of surfactants on the aggregation state of amphotericin B, Biochim Biophys Acta 1030 (1990) 289-295.
[35] I. Blanc, M. Bueno Da Costa, J. Bolard, M. Saint-Pierre Chazalet, Oligonucleotide delivery by a cationic derivative of the polyene antibiotic amphotericin B. I: interaction oligonucleotide/vector as studied by optical spectroscopy and electron microscopy, Biochim Biophys Acta 1464 (2000) 299-308.

[36] J. Barwicz, S. Christian, I. Gruda, Effects of the aggregation state of amphotericin B on its toxicity to mice, Antimicrob Agents Chemother 36 (1992) 2310-2315.
[37] K. Wojtowicz, W.I. Gruszecki, M. Walicka, J. Barwicz, Effect of amphotericin B on dipalmitoylphosphatidylcholine membranes: calorimetry, ultrasound absorption and monolayer technique studies, Biochim Biophys Acta 1373 (1998) 220-226.
[38] W.I. Gruszecki, M. Gagoś, P. Kernen, Polyene Antibiotic Amphotericin B in Monomolecular Layers: Spectrophotometric and Scanning Force Microscopic Analysis, FEBS Lett. 524 (2002) 92-96.
[39] J. Minones Jr., C. Carrera, P. Dynarowicz-Latka, J. Minones, O. Conde, R. Seoane, J.M. Rodriguez Patino, Orientational Changes of Amphotericin B in Langmuir Monolayers Observed by Brewster Angle Microscopy, Langmuir 17 (2001) 1477-1482.
[40] S. Feng, Interpretation of mechanochemical properties of lipid bilayer vesicles from the equation of state or pressure-area measurement of the monolayer at the air-water or oil-water interface, Langmuir 15 (1999) 998-1010.
[41] J.F. Nagle, Theory of lipid monolayer and bilayer phase transitions: Effect of headgroup interactions, J. Membrane. Biol. 27 (1976) 233-250.
[42] M. Kasha, H.R. Rawls, M. Ashraf El-Bayoumi, The exciton model in molecular spectroscopy, Pure Appl. Chem. 11 (1965) 371-392.
[43] J. Parkash, J.H. Robblee, J. Agnew, E. Gibbs, P. Collings, R.F. Pasternack, J.C. de Paula, Depolarized Resonance Light Scattering by Porphyrin and Chlorophyll a Aggregates, Biophys. J. 74 (1998) 2089-2099.
[44] B. De Kruijff, W.J. Gerritsen, A. Oerlemans, R.A. Demel, L.L. van Deenen, Polyene antibiotic-sterol interactions in membranes of Acholeplasma laidlawii cells and lecithin liposomes. I. Specificity of the membrane permeability changes induced by the polyene antibiotics, Biochim. Biophys. Acta 339 (1974) 30-43.

Figure captions

Fig. 1 Chemical structure of amphotericin B

Fig. 2 (A) Schematic representation of the experimental set-up applied to measure light absorption by a monomolecular layer formed with amphotericin B and (B) representation of amphotericin B molecule, its transition dipole moment vector (μ) and the projection of the transition dipole vector on the plane of the monolayer (the plane xy). Gray bar represents the chromophore. Measuring light was directed along the z axis. $E_{\perp}$ and E_{II} represent the electric vectors of light polarized perpendicular and parallel with respect to the direction of monolayer compression (along x axis).

Fig. 3 Isotherm of compression of amphotericin B monomolecular layer deposited at the argon-water interface. Lines fitted to the linear portions of the isotherm extrapolated to zero surface pressure point the specific molecular area values for molecules oriented horizontally (148 $Å^2$/molecule) and vertically (36 $Å^2$/molecule) with respect to the plane of the monolayer. The inset presents horizontal and vertical orientation of molecules in the monolayer.

Fig. 4 Light absorption spectra of monomolecular layer of amphotericin B deposited at the argon-water interface before compression (A) and compressed to the surface pressure 25 mN/m (B) and 32 mN/m (C). The components of Gaussian deconvolution of the spectra are shown with thin lines and the fit superimposed on the spectra are shown with thick lines.

Fig. 5 Diagram of localization of the energy levels of amphotericin B in monomeric form (vibrational levels 0-0, 0-1, 0-2) and dimeric form, based on the results of the Gaussian deconvolution of the absorption spectra (Fig. 4). Individual energy levels correspond to the spectral bands as assigned in Tab. I. The observed splitting of the energy levels $2\beta_1$ and $2\beta_2$ enabled determination of the dipole-dipole interaction energies β_1=890 cm^{-1} and β_2=3741 cm^{-1} and distances between the centers of chromophores of neighboring molecules R_1 and R_2 as schematically depicted in the inset. Grey circles represent projections of the chromophores of amphotericin B on the plane of the monolayer. Each vibrational energy level of AmB in the monomeric form is shifted toward lower and higher energies by the values corresponding to the dipole-dipole interaction energies β_1 and β_2.

Fig. 6 Surface pressure dependencies of absorbance level of monomolecular layer of amphotericin B recorded at 409 nm, corresponding mainly to the monomeric form (A) and at 353 nm, corresponding to the dimeric form (B). Panel C presents the absorbance ratio from the panels A and B and represents the surface pressure dependency of changes in the monomer to dimer ratio (filled circles) superimposed on the isotherm of compression (solid line).

Fig. 7 (A) Surface pressure dependencies of absorbance level of monomolecular layer of amphotericin B recorded at 409 nm with light polarized parallel (A_{II} open circles) and perpendicular ($A_{\perp}$ filled circles) with respect to the direction of compression. (B) Surface pressure dependency of $\langle\cos^2\phi\rangle$ where ϕ is the azimuth angle between the monolayer compression direction and the projection of the transition dipole moment vector on the plane of the monolayer. The inset shows the proposition of molecular arrangement in the monolayer at the surface pressure 20 mN/m (a) and higher surface pressure values (b).

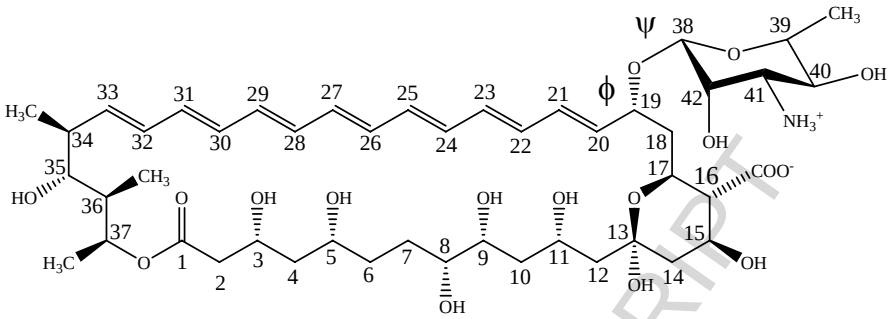

Fig. 1 Gagos and Gruszecki

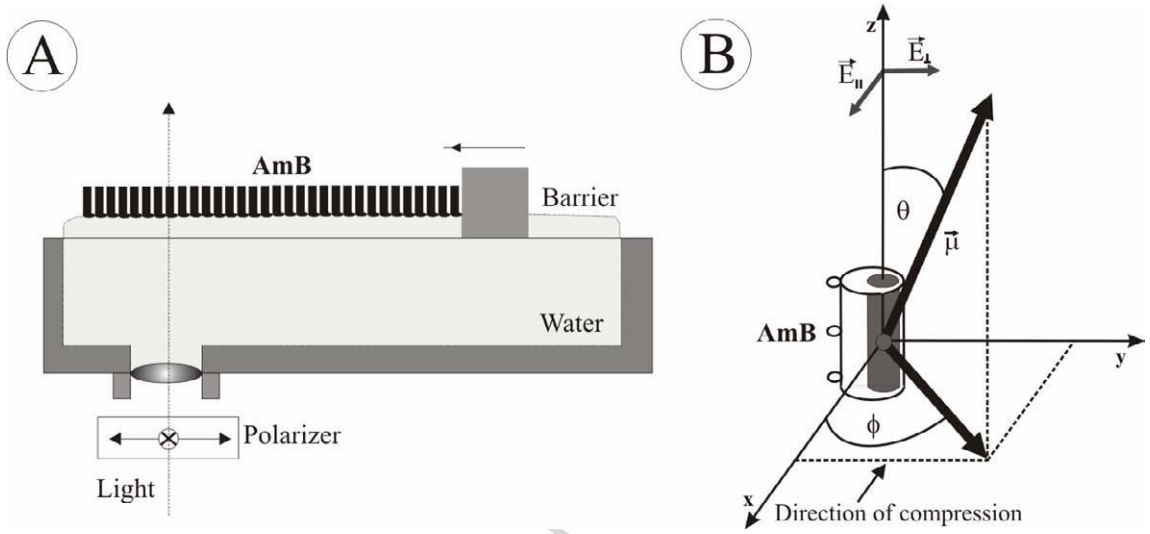

Fig. 2 Gagos and Gruszecki

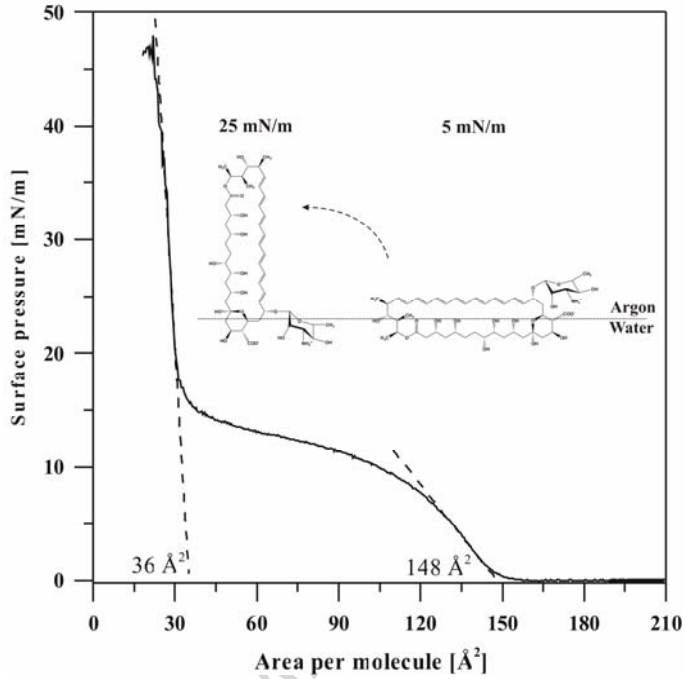

Fig. 3 Gagos and Gruszecki

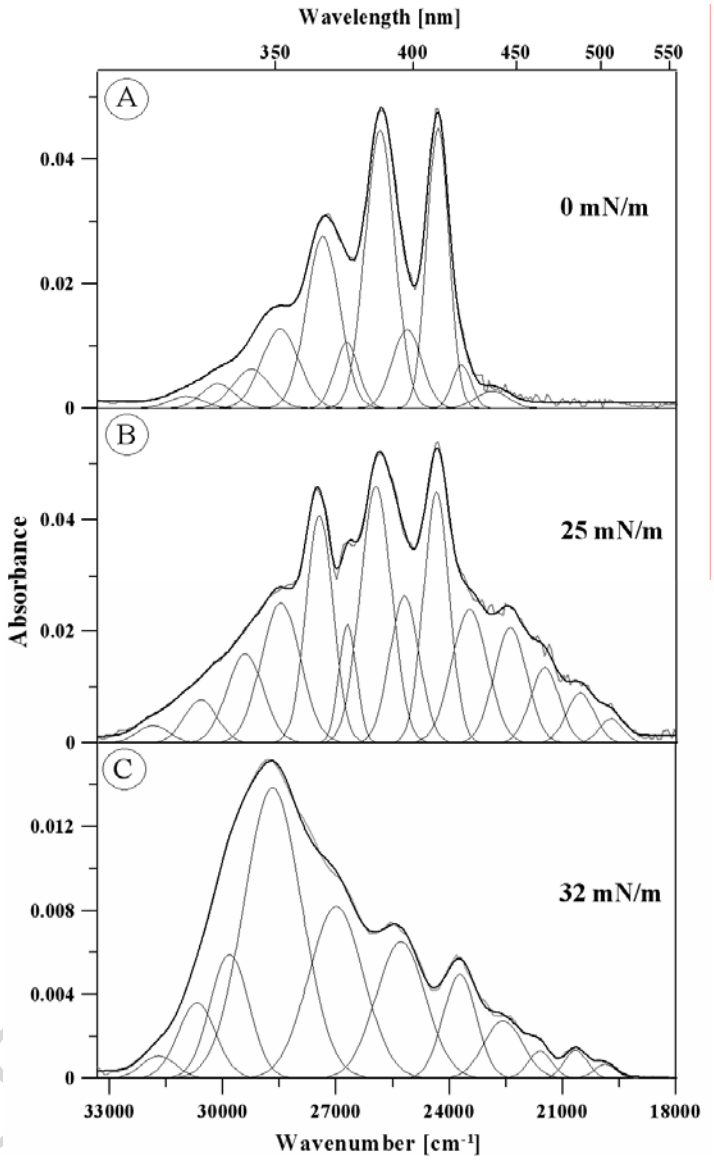

Fig. 4 Gagos and Gruszecki

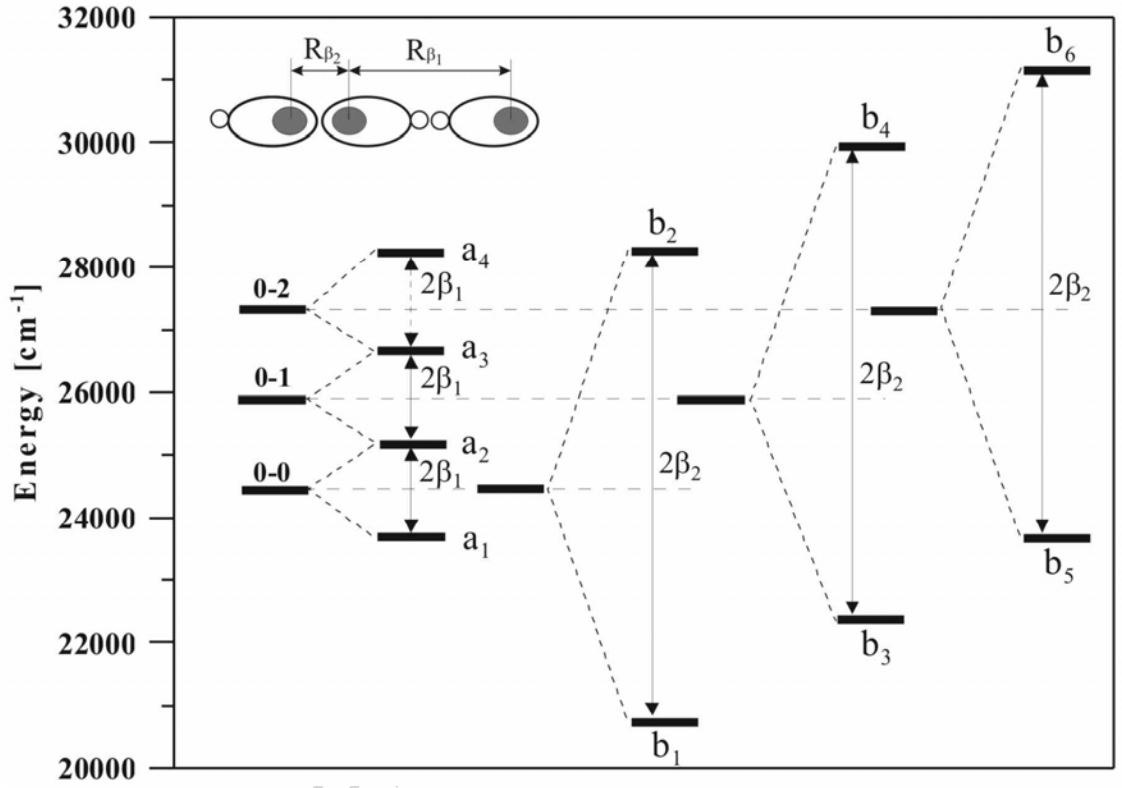

Fig. 5 Gagos and Gruszecki

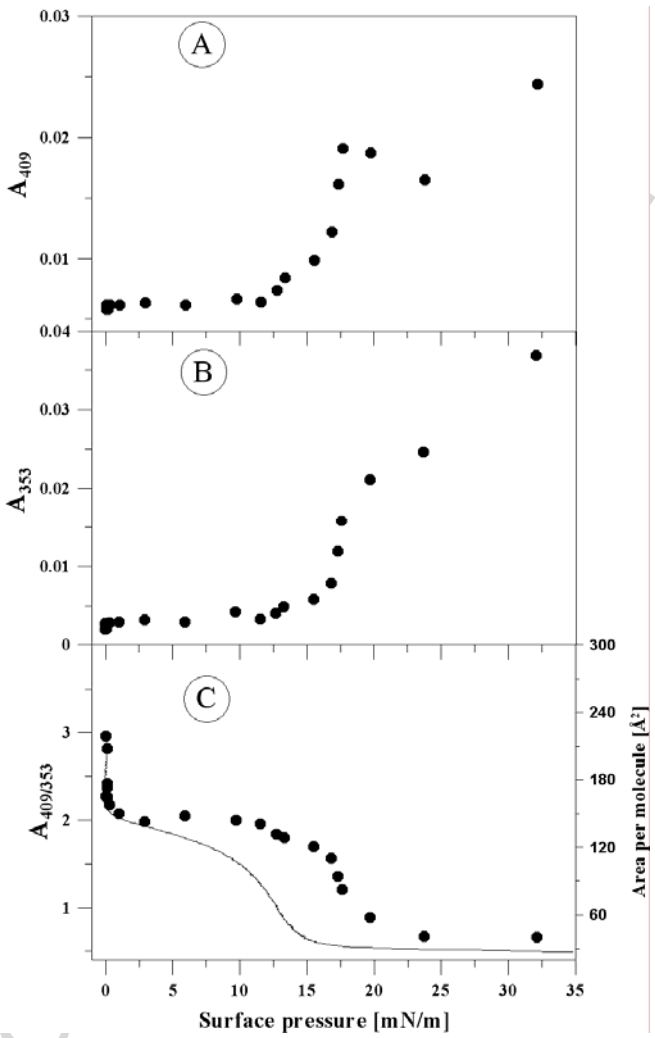

Fig. 6 Gagos and Gruszecki

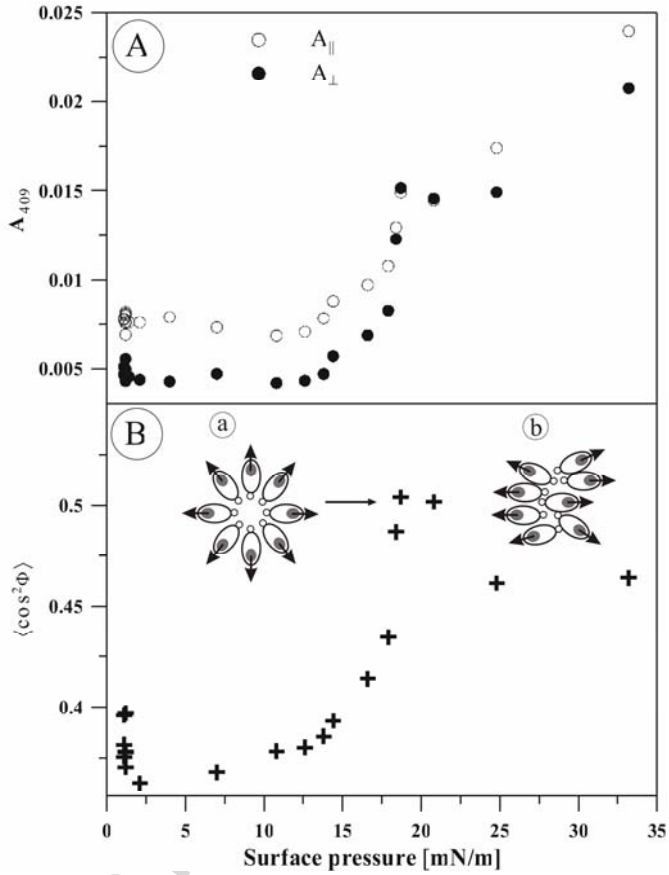

Fig. 7 Gagos and Gruszecki

Table I
Parameters of Gaussian deconvolution of absorption spectra recorded from amphotericin B monomolecular layers at different surface pressures (Fig. 4). The assignment of the bands corresponds to the energy level diagram presented in Fig. 5.

Surface pressure [mN/m]	**Gaussian component**			
	N_o	**Position**		**assignment**
		[cm^{-1}]	[nm]	
0	1	31041	322	b_6
	2	30198	331	b_4
	3	29308	341	-
	4	28571	350	a_4, b_2
	5	27439	364	0-2
	6	26804	373	a_3
	7	25946	385	0-1
	8	25226	396	a_2
	9	24420	409	0-0
	10	23802	420	a_1, b_5
	11	23029	434	-
25	1	31928	313	-
	2	30689	326	b_6
	3	29522	339	b_4
	4	28568	350	a_4, b_2
	5	27541	363	0-2
	6	26799	373	a_3
	7	26057	384	0-1
	8	25295	395	a_2
	9	24452	409	0-0
	10	23585	424	a_1, b_5
	11	22532	444	b_3
	12	21637	462	-
	13	20691	483	b_1
	14	19903	502	-
32	1	31696	315	-
	2	30688	326	b_6
	3	29831	335	b_4
	4	28690	349	a_4, b_2
	5	26998	370	a_3
	6	25287	395	a_2
	7	23729	421	a_1, b_5
	8	22569	443	b_3
	9	21599	463	-
	10	20649	484	b_1
	11	19869	503	-